Theoretical and Experimental Drawdown Pore Pressures in Porous Embankments

by

D. C. GREEN, B.E., B.Com., M.Eng.Sc., M.I.E.Aust.

Engineer, Civil and Architectural Department, State Electricity Commission of Victoria

K. G. MILLS, B.E., M.Eng.Sc.,

Lecturer in Civil Engineering, University of Queensland

and

P. J. MOORE, B.E., M.S., Sc.D., M.I.E.Aust.

Reader in Civil Engineering, University of Melbourne

SUMMARY: The development and verification are described of a finite element computer program for solution of problems of two-dimensional Darcian seepage flow with particular application to evaluation of pore pressures in embankments during and after reservoir drawdown. The program was used to compare theoretical pore pressures with pore pressures measured during an extensive series of drawdown tests on model dam embankments constructed of two different sands. An attempt was also made to compare pore pressures predicted, using the finite element program, with measured values reported in the literature for two actual dams. Conclusions are then drawn regarding the usefulness of the program.

1 INTRODUCTION

In assessing the stability of the upstream slope of an embankment during reservoir drawdown, a reliable technique is necessary for calculation of the pore water pressures in the soil forming the embankment. For a relatively slow drawdown and an embankment of coarse grained soils such as sands and gravels, it is widely accepted that the pore pressures are determinable from considerations of unsteady seepage (Refs. 1, 2). For a relatively rapid drawdown and an embankment of fine grained soils such as silts and clays, the pore pressure changes are determined from considerations of stress relief following the removal of the water load from the upstream face (Ref. 3). For a relatively rapid drawdown (including those so rapid that embankment failure may be initiated) and an embankment of coarse grained soil, it is not clear which procedure should be used for pore pressure determination. Therefore (for example) the designer of dams with substantial zones of coarse-grained materials such as might be used to impound pumped storage or hydro-electric reservoirs subject to drawdowns as rapid as several metres per day, or faster, faces uncertainty. To clarify this matter, an investigation was commenced to examine the extent to which the pore pressures may be calculated by means of a Darcian seepage model.

2 ANALYSIS BY FINITE ELEMENT PROGRAM

A computer program was developed which employs the finite element procedure to solve for the seepage flow pattern in an embankment during and after drawdown of the upstream water level (Ref. 4). This technique, which is now widely known, is expounded in Ref. 5. The analysis was confined to two-dimensional flow, which can be described by Darcy's Law, through isotropic or anisotropic material. Capillary effects are neglected.

The region of the embankment through which seepage flow occurs is divided into a number of triangular elements and the total head is computed at each node. The variation of total head over any triangle is expressed as a "linear function" of the three (unknown) nodal values. The flow velocity in the element, being related to the gradient of this function, is then written in terms of the nodal total heads, the elemental geometry and permeability. For each node, an equation of continuity is set up by considering the flow velocities in the contingent elements. Assuming the soil matrix and the pore fluid to be incompressible, and given the boundary conditions at any time "t", a complete set of simultaneous equations in the unknown nodal heads can be formulated. This is then solved for all the nodes in the mesh.

During drawdown, the upper seepage line is in motion; its displacement velocity dn/dt, where n is normal to the line, is related to the normal component, V_n, of the discharge velocity by the equality:

$$\frac{dn}{dt} = \frac{V_n}{n_e}$$

where n_e is the effective or active porosity of the soil matrix (defined in Section 2(b)).

This equation determines the displacement velocity of the phreatic line at the instant of time, t. The rate of translation is used to locate the line at a later time $(t + \Delta t)$, and the steady seepage equations are reformulated to compute the corresponding distribution of total head at this time. The whole cycle of calculations is repeated for a new increment of time, Δt, with any appropriate changes to the boundary conditions, such as the change in reservoir level. This procedure is sometimes known as the method of "successive steady states". The time "t", becomes a parameter for each solution rather than a variable.

For overall computational efficiency and ease of programming, the finite element mesh is drawn with nodes in vertical lines. Thus as the top seepage boundary translates, the nodes on it move vertically until they coalesce with the nodes immediately below, elements being first modified and then deleted progressively. The program uses Gauss-Seidel iteration for the total head solution. This was considered most effective because the redundant (i.e. deleted) nodes are easily catered for and good starting approximations exist from the previous time step.

In order to verify the program the numerical computations were checked by comparison with the experimental work of Browzin (Ref. 6). His study was performed in a Hele-Shaw flume (viscous flow model), and so is compatible with the program's assumptions of incompressibility of the pore fluid and the soil matrix. The agreement was remarkably good, so the program was considered to be reliable.

3 EXPERIMENTS WITH MODEL EMBANKMENTS

(a) Outline of Experiments and Instrumentation

To gain data concerning the rate of dissipation of pore pressure in earth-rock dams subject to unusually rapid rates of reservoir drawdown, model dam embankments were constructed from sand and were instrumented with pressure transducers to measure pore water pressure (Ref. 7). The measured pore pressures were compared with those predicted using the finite element program referred to above.

The embankments were constructed in the shape of a right-angled triangle in section against the vertical end-wall of a steel tank 4.72 m long, 1.22 m wide and 0.78 m high, with a glass panel on each side. To saturate the embankment, the tank was filled with water by pumping from a large sump. Reservoir drawdown was achieved by removing a plug from an outlet pipe of 152 mm diameter set in the floor of the tank at the end furthest removed from the embankment and discharging through a gate valve (see Fig. 1).

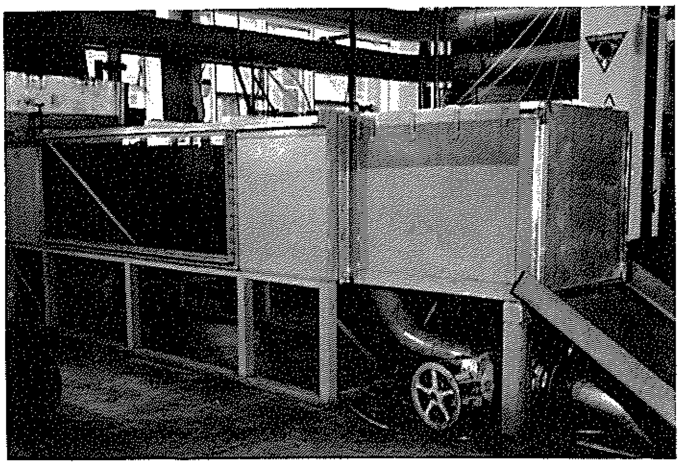

Fig. 1 Test tank for model embankments

The rates of drawdown were controlled by presetting the opening of the gate valve, after calibrating it with a dummy embankment in place in the tank. The location of the valve relative to the tank floor was carefully chosen so as to yield a rate of drawdown which was very nearly constant over the full range of water levels used, except for the last 20 mm to 50 mm, when vortex formation caused a slowing down of the discharge. All embankments used were 0.75 m high and were subjected to complete drawdown in times ranging from 8.5 hours to 50 seconds by this means. An alternative discharge arrangement in the form of a sliding vertical gate in the end of the tank (see Fig. 1) allowed extremely rapid drawdown to be achieved, the fastest rate used being achieved in 17 seconds.

Six embankments were tested in this tank, with slopes of 1:1.5, 1:2.0 and 1:2.5, using two different sands. Pore pressures within each embankment were measured in selected locations on the centreline section using Tyco Bytrex AB-15 submersible pressure transducers fitted with a protective cap of BSS No. 50 brass mesh. The overall diameter (including cap) was 26 mm and the length of the main body 27 mm.

For almost half of the tests, five transducers were implanted in the embankments, but after one failed, only four were used in the remaining tests. In all tests, a further transducer was mounted in the floor of the tank away from the embankment to measure water level. In all but the fastest drawdowns a "manual" record of water level was also made during tests by reading from a measuring tape fixed to one of the glass panels in the tank. All transducers were connected via an attenuation and balancing circuit to a Southern Instruments Model 1100 six-channel ultra-violet recorder, which produced a trace from each transducer output on paper 120 mm wide. The system was calibrated before and after the series of tests carried out on each embankment, by inserting the transducers in a battery of six water pressure chambers connected to a manometer into which water could be pumped to controlled height.

(b) Material Properties

Two different sands were used for the embankments as follows:

(i) Garfield Sand: This was a rounded to subrounded gravelly coarse quartz sand, without fines (Unified Classification, SP).

(ii) Plaster Sand: This was a medium-to-coarse yellow sand with very little fines, and with subangular particles (Unified Classification, SP).

The grading characteristics are given in Fig. 2.

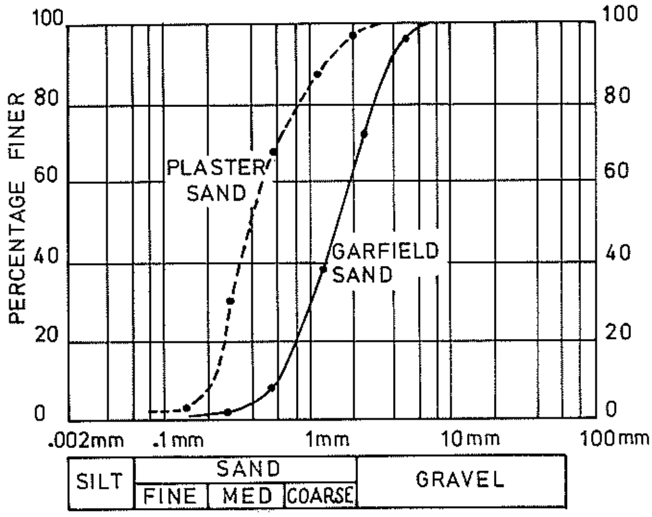

Fig. 2 Grading curves for materials in model embankments

A series of tests was carried out to determine the (Darcy) coefficient of permeability as a function of void ratio for each material. Tests were performed with vertical flow at constant head in cylindrical steel cells of 203 mm diameter on samples compacted in three layers to a thickness of about 150 mm, and a range of head gradients up to 1.8 was used. Some scatter was experienced in the results, and some non-linearity of flow was noted, particularly in Garfield Sand, but for practical purposes the coefficient of permeability was taken as a function of void ratio alone. Several attempts were made to measure the horizontal coefficient of permeability, but results were inconclusive, and both materials were regarded as hydraulically isotropic in subsequent analysis.

The effective porosity was defined as the volume of water freely drainable from a unit volume of soil initially saturated (after Ref. 8). The average value of this parameter for a given void ratio was calculated by allowing the sample to drain at the conclusion of each vertical permeability test.

The properties of embankments used in the drawdown tests are summarised in Table 1.

TABLE 1

PROPERTIES OF EMBANKMENTS IN DRAWDOWN TESTS

Test Series	Material	Slope	Mean Void Ratio e	Relative Density D_R	Mean Porosity n	Effective Porosity n_e	Mean Moisture Content (as placed) w%	Coeff. of Permeability k m/s
T1-T15	Garfield Sand	1:2.0	0.80	0.19	0.45	0.33	4.0	7.2×10^{-3}
T16-T26	" "	1:1.5	0.76	0.26	0.43	0.29	4.6	6.2×10^{-3}
T27-T38	" "	1:2.5	0.72	0.33	0.42	0.26	4.0	5.2×10^{-3}
T42-T49	Plaster Sand	1:2.5	0.66	0.56	0.40	0.15	4.7	1.5×10^{-4}
T50-T58	" "	1:2.0	0.64	0.59	0.39	0.12	9.5	1.3×10^{-4}
T59-T66	" "	1:1.5	0.51	0.83	0.34	0.03	10.6	4.1×10^{-5}

(c) Comparison of Measured and Computed Pore Pressures

Of the total of sixty-three drawdown tests referred to in Table 1, thirty-five were performed at rates of drawdown which caused failure of the banks, and twenty-eight were performed at slower rates. Ten of the former category and thirteen of the latter were simulated mathematically using the finite element program referred to above. Both the "failure" cases and the "non-failure" cases simulated contained representatives of each of the six embankments tested. A finite element mesh was devised for each embankment section drawn to scale, with transducer locations coinciding with element nodes. The reservoir drawdown data was formulated as a series of steps by specifying the times at which the actual water level during each test reached the level of each successive node of the face of the embankment. The number of such steps ranged from thirteen to fifteen, depending on the details of the mesh.

The computed pore pressure heads at the end of each drawdown "step" for those nodes corresponding to transducer locations were plotted up to the time when drawdown was complete (the program was capable of producing results beyond this time, but use was not made of this facility). A comparison was then made between measured and computed pore pressures for each transducer in each test.

An example of such a comparison is given in Fig. 3. While Fig. 3 is only an example for illustrative purposes, and should not be taken to embody all features of the many comparisons made in this manner, the following general results were obtained:

(i) In every test series (a "series" comprising all tests on an embankment at given slope in a given material) the agreement between measured and computed pore pressure was better for tests in which failure did not occur than for those in which failure occurred. For "failure" tests, however, agreement up to the onset of failure was just as good as that achieved for "non-failure" tests. This was to be expected since Darcy seepage theory takes no account of pore pressure changes which may occur at failure. Computed pore pressures became higher than measured pore pressures after failure, apparently on this account.

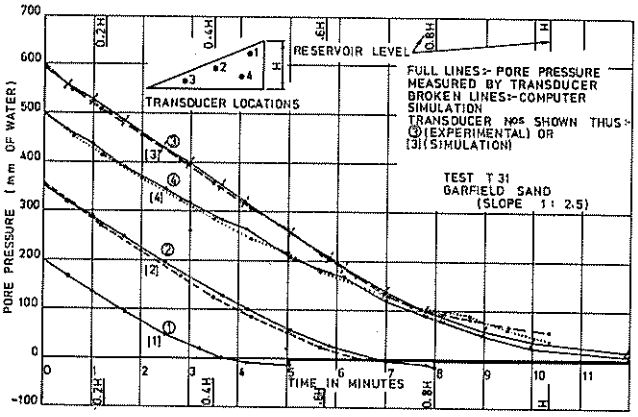

Fig. 3 Example of comparison of measured and computed pore pressures for model embankments (non-failure case)

(ii) For every test series, agreement was considerably better for the earlier part of the drawdown compared with the later portion.

(iii) For non-failure tests, in the first 50% of dissipation of initial pore pressure, discrepancies between measured and computed pore pressure heads generally ranged from 0 to 10 mm. Depending on the location of the transducers, this represented errors ranging from zero to about 10%. In the second 50% of dissipation, discrepancies generally ranged from 5 to 20 mm, and hence the percentage errors were considerably greater, particularly when low pore pressures were recorded.

(iv) For failure tests, in the first 50% of dissipation of initial pore pressure, discrepancies generally ranged from 5 to 10 mm, or from about 5% to 10%, depending on the location of the transducers concerned. In the second 50% of dissipation, discrepancies generally ranged from 10 to 25 mm, representing even greater percentage "errors" than for the corresponding stages of drawdown for the non-failure cases.

(v) While (iii) and (iv) above applied generally, it was noted that whenever pore pressure heads below about 150 mm were recorded discrepancies ranged from about 15 to 50 mm (i.e. up to about 40%).

(vi) In no case did the computed pore pressure head indicate a negative value (since capillary effects were ignored in the theory), whereas negative values were recorded by the transducers, ranging from a "maximum" of -50 mm in Garfield Sand to a "maximum" of -160 mm in Plaster Sand.

With regard to the recorded negative pore pressures mentioned above, it was observed that transducers used to measure water level outside the bank often overestimated at levels lower than about 150 mm to 200 mm, and that at very low levels (less than about 50 mm) the level measured in this way was sometimes up to 200% in error. The transducers were at the very lowest level of their rated range at such pressures and on this account they were regarded with some suspicion. Nevertheless, examination of all the results showed that negative pressures of greater magnitude were consistently found in the finer sand than in the coarser one, and certain other observations also led to the conclusion that real negative pore pressures did occur once the reservoir level fell below the level of the transducers, although the exact magnitude of these pressures was in doubt. The conclusion was that the majority of the greater discrepancy between measured and computed pore pressures in the lowest range of pore pressures at any location was due to capillarity effects rather than to unreliability of the transducers.

4 COMPARISONS WITH BEHAVIOUR OF ACTUAL DAMS

(a) General

Although the finite element program was verified, its basic assumptions may limit its applicability in the study of real structures. Errors may occur with fine-grained materials owing to capillarity or volume change of the soil, and with coarse-grained materials due to non-Darcian flow. It has already been noted also that for a fully saturated fine-grained and relatively impermeable embankment, the pore pressures would not be determinable from seepage considerations at all; instead, pore pressure changes should be calculated by means of the pore pressure parameter $\bar{B}$ (Ref. 3).

There is a dearth of documented examples of drawdown of real dams in which sufficient quantitative data is given for the behaviour to be simulated mathematically, and no suitable examples could be found for real embankments in coarse-grained materials. However, the finite element program was applied to two field situations where adequate data was reported in the literature, in order to illustrate the extent to which a Darcian seepage model may be used to determine drawdown pore pressures in actual dams.

(b) Glen Shira Dam (Ref. 9)

This structure is a relatively low embankment of morainic fill with a concrete core wall and a rockfill shell on the upstream slope. Calculations suggest that at the end of the reported drawdown, the pore pressures generated will not have dissipated. Fig. 4 shows a typical result of pore pressures predicted by the finite-element program. There is an appreciable time lag between observed and predicted pore pressures, though possibly some of this arises from a lag inherent in the instrumentation itself. The computed values at all the piezometer tips were within a metre of the measured values one to two days after the end of the drawdown period.

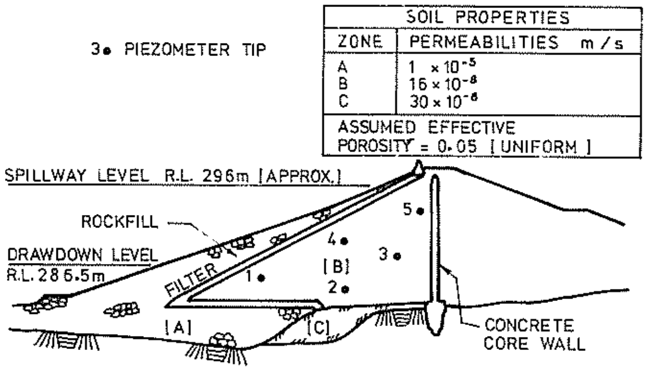

(a) Cross-section showing location of piezometers

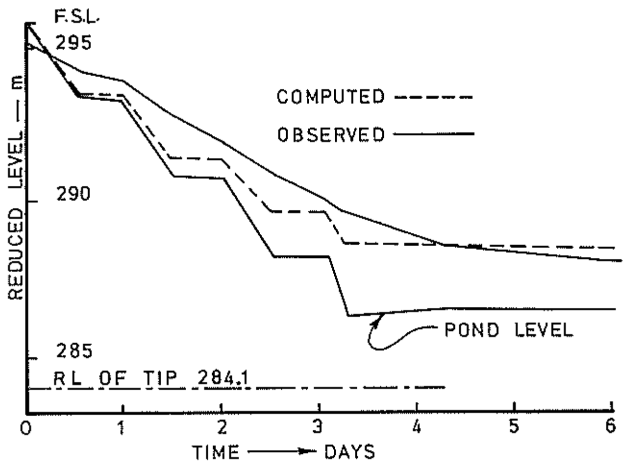

(b) Example of comparison of measured and predicted piezometric levels (piezometer No. 2)

Fig. 4 Glen Shira Dam

(c) Rocky Valley Dam (Ref. 10)

This is an earth-rock dam about 30 m high. As in the previous example, calculations indicated that significant stress-dependent pore pressures were present during the reported drawdown of 9.5 m in 60 days. Fig. 5 shows the observed and computed values of pore pressure at the end of drawdown. The two sets of values agree well near the base of the structure, but differ considerably for the upper row of piezometers.

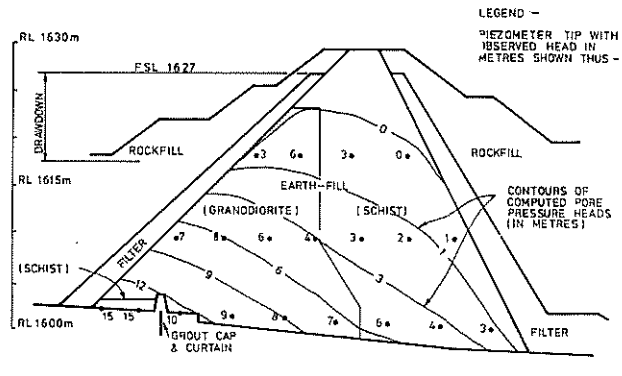

Fig. 5 Rocky Valley Dam – comparison of measured and computed drawdown pore pressures

Further consideration has shown that compressibility due to partial saturation and occlusion of pores by air may also be significant in this embankment's reported behaviour. The finite element program was also used to compare "steady seepage" observations with computed values of pore pressure. Good agreement was obtained when a ratio of five to one for the horizontal and vertical permeability coefficients was used in the computations.

5 CONCLUSIONS

For model embankments built of sandy soils reasonable agreement was obtained between the observed pore pressures during drawdown and those calculated by means of the finite element program, which was based upon Darcian seepage flows. When failure of the embankments occurred the calculated pore pressures were greater than those observed. Agreement should not be expected under failure conditions, however, since the program does not take stress dependent pore pressures into account.

The application of the finite element program to full-scale structures is limited to cases where the pore pressures are determinable from Darcian seepage considerations. In cases where embankments are composed of fine-grained soils where stress dependent pore pressures are likely to be predominant during drawdown, this finite element program should not be used. Similar caution should be exercised in any situation where capillary effects may be significant.

6 ACKNOWLEDGEMENT

The sponsorship of the experimental work on the model embankments, referred to herein, by the State Electricity Commission of Victoria, is gratefully acknowledged.

7 REFERENCES

1. CASAGRANDE, A. Seepage Through Dams. Journal of New England Water Works Association, June, 1937. Reprinted in Contributions to Soil Mechanics, 1925-1940, Boston Society of Civil Engineers, 1940, pp. 295-336.

2. REINIUS, E. The Stability of the Upstream Slopes of Earth Dams. Swedish State Committee for Building Research (Meddelanden Stratens Kommitté for Byggnadsforkning) Bull. No. 12 (1949).

3. BISHOP, A.W. The Use of Pore Pressure Coefficients in Practice. Geotechnique, Vol. 4, No. 4, 1954, pp. 148-152.

4. MILLS, K.G. Computation of Post-Drawdown Seepage in Earth Dams by Finite Elements. Thesis (M.Eng.Sc.), Department of Civil Engineering, University of Queensland, Brisbane, 1970.

5. ZIENKIEWICZ, O.C. and CHEUNG, Y.K. The Finite Element Method in Continuum Mechanics, McGraw-Hill, 1967.

6. BROWZIN, B.S. Non-Steady-State Flow in Earth Dams After Rapid Drawdown. Proc. 5th Int. Conf. on Soil Mech. and Found. Eng. (Paris, 1961), Vol. 2, pp. 551-554.

7. GREEN, D.C. Drawdown Pore Pressures in Rockfill. Thesis (M.Eng.Sc.), Department of Civil Engineering, University of Melbourne, 1972.

8. NEWLIN, C.W. and ROSSIER, S.C. Embankment Drainage After Instantaneous Drawdown, Journal of Soil Mech. and Found. Eng. Division, A.S.C.E., Vol. 93, No. SM6, November, 1967, pp. 79-95.

9. PATON, J. and SEMPLE, N.G. Investigation of the Stability of an Earth Dam, Including Details of Pore Pressure Recorded During a Controlled Drawdown Test. Proc. Conf. on Pore Pressure and Suction in Soils, London, 1960 (Butterworths, 1961), pp. 85-90.

10. McKENZIE, R.J. Pore Pressure and Settlement Observations at Rocky Valley Dam, Proc. 3rd Australia-New Zealand Conf. on Soil Mech. and Found. Eng. (Sydney, 1960), pp. 5-10, and pp. 235-236.